Natural radioactivity levels (K, Th, U and Rn) in the Cecita Lake area (Sila Massif, Calabria, Southern Italy): an attempt to discover

Geoderma 152 (2009) 145–156

Contents lists available at ScienceDirect

Geoderma

journal homepage: www.elsevier.com/locate/geoderma

Natural radioactivity levels (K, Th, U and Rn) in the Cecita Lake area (Sila Massif, Calabria, Southern Italy): An attempt to discover correlations with soil features on a statistical base

A. Buccianti [a,*], C. Apollaro [b], A. Bloise [b], R. De Rosa [b], G. Falcone [c], F. Scarciglia [b], A. Tallarico [c], G. Vecchio [d]

[a] Dipartimento di Scienze della Terra, Università degli Studi di Firenze, Via G. La Pira 4, 50121 Firenze, Italy
[b] Dipartimento di Scienze della Terra, Università della Calabria, Ponte Bucci 15-B, 87036, Arcavacata di Rende, Cosenza, Italy
[c] Dipartimento di Fisica, Università della Calabria, Ponte Bucci 31-C, 87036, Arcavacata di Rende, Cosenza, Italy
[d] Istituto Sperimentale per lo Studio e la Difesa del Suolo (ISSDS), 88063 Catanzaro Lido, Cosenza, Italy

ARTICLE INFO

Article history:
Received 6 January 2009
Received in revised form 14 May 2009
Accepted 31 May 2009
Available online 26 June 2009

Keywords:
Natural radioactivity
Soil features
Soil gas
Compositional data analysis

ABSTRACT

Soils can exhibit a complex range of physical, mineralogical, and chemical features depending on many interrelated factors such as parental rock composition and mineralogy, climate, topography, vegetation amounts and types, water infiltration versus runoff, soil moisture, organic matter, presence and types of anthropogenic contaminants, and many others. Radioactivity as measured on these complex systems is consequently perturbed by several mixed effects. In order to find out a possible (potential) relationship among soil properties and experimental data attributable to radioactivities of K, Th, U and Rn a detailed investigation has been performed in the Cecita Lake basin (Sila Grande, Calabria, Southern Italy). Most of the soil types outcropping in the Cecita Lake surroundings belong to the Entisol and Inceptisol orders [USDA (United States Department of Agriculture), 2006. *Keys to Soil Taxonomy*. 10th edit., USDA, Soil Survey Staff, Natural Resources Conservation Service, Washington D.C., 333 pp.], representing relatively young, poorly to moderately differentiated soils, showing features strongly dependent on the nature of the parent rock and the climatic conditions.

Disintegrations contributed by K, Th, U and Rn measured respectively in % (K), ppm (U and Th) and kBq/m^3 (Rn), have been related to 13 a priori known soil unit groups with well-defined general features and spatial position. The data have been analysed by using graphical and numerical statistical procedures able to manage compositional data in a correct sample space. The paper summarises the results of this research and highlights the conclusions drawn from these investigations, particularly concerning i) the modelling of the high U variability, a behaviour that tends to homogenise the differences potentially attributable to soil features, with the exception of situations where uranium could be enriched due to adsorption onto iron oxi-hydroxides and/or clay minerals or concentrated in argillic horizons due to illuviation; ii) the discovering of the discriminative effect of the K/Th ratio values, particularly for soil groups where Th behaviour, as other tetravalent actinides, is strongly affected by the presence of mineral colloids or where the presence of clays affects the trapping of K; iii) the clustering of the a priori known soil groups in four new sets characterised by internal similarities for Rn values for which the morphology appears to be the most important discriminative effect.

1. Introduction

Developing and implementing research about natural radioactivity involves a complex set of actions such as collection of samples, measurements carried out in the field and laboratory, data evaluation and environmental modelling. This type of investigation increases the knowledge on the behaviour of the isotopes in natural cycles and, in particular, in the superficial environment (Badr et al., 1993; Lima et al., 2005). In this context the main role played by soils, as compared with those of the underlying rocks, has been recognised since they contribute more than 90% of Rn in houses (Akerblom et al., 1984; Nero et al., 1990).

Radioactivity is defined as the spontaneous breakdown of a nucleus. The unstable, or radioactive, ones decompose by emitting a small particle that usually carries a great deal of energy. The biological effects related to the passage of these radiations through the cells are due to changes in their chemistry caused by ionization, excitation, dissociation, and atomic displacement. Very heavy elements are particularly prone to this type of decomposition and the particles emitted in these cases are usually either alpha (an helium nucleus) or beta (an electron) in character. The radioactive decomposition of the

* Corresponding author. Tel.: +39 055 2757493; fax: +39 055 284571.
E-mail address: antonella.buccianti@unifi.it (A. Buccianti).

0016-7061/$ – see front matter © 2009 Elsevier B.V. All rights reserved.
doi:10.1016/j.geoderma.2009.05.027

atoms does not occur all at once. A measure often used to express such decomposition rates is the time period required for half the nuclei in a sample to disintegrate, called its half-life, $t_{1/2}$, describing an exponential type of decay.

Radioactive isotopes in the environment come from both natural sources (K, Th, U and Rn in rocks, minerals and soils) and anthropogenic sources (bomb testing, nuclear medicine, nuclear accidents and nuclear fuel cycle). All the naturally occurring heavy radioisotopes, i.e. those with atomic numbers of 82 (lead) and larger, are members of a radioactive decay series commencing with one of the three radionuclides ^{238}U, ^{235}U and ^{232}Th. The series terminates with one of the stable isotopes of lead ^{206}Pb, ^{207}Pb and ^{208}Pb with a half-life of about 14.05×10^9 years (Nelson-Eby, 2004; Siegel & Bryan, 2005).

Most of the heat which presently flows through the earth crust can be attributable to the presence of ^{238}U, ^{232}Th and ^{40}K and the natural background radiation on the Earth's surface is also largely due to the presence of these radioactive elements and their decay products. Potassium is an alkaline element, with volatile and lithophile behaviour, so that its concentration in the Earth is poorly constrained. The K^+ ion is very large and although it may enter octahedral sites, it often fits 12-coordinated sites as in feldspars and micas. During melting in the mantle and basalt differentiation K is strongly incompatible and follows other incompatible elements such as Th and U, thus cumulating in felsic igneous melts. The naturally occurring isotopes of potassium are ^{39}K (93.1%), ^{40}K (0.0119%) and ^{41}K (6.9%). ^{40}K is radioactive with a half-life of 1.27×10^9 years, and its decay is characterised by K-electron capture or β^- processes.

Uranium is preferentially concentrated in the Earth's crust and there is a relationship between the type of igneous rock and its uranium content (Plant et al., 2003). Acid igneous or granitic rocks have the highest concentrations (2–10 mg kg^{-1}), basaltic rocks contain lower concentration (0.3–0.8 mg kg^{-1}) while the concentrations in sedimentary rocks show a wide range.

Thorium is characterised by twenty seven radioisotopes with the most abundant and/or stable being ^{232}Th with a half-life of about 14.05 billion years. Other important isotopes are ^{230}Th with a half-life of 75,380 years, ^{229}Th with a half-life of 7340 years and ^{228}Th of 1.92 years. All of the remaining radioactive isotopes have a half-life that is less than thirty days and the majority of these have half-life that are less than 10 min. Thorium is a lithofile element that does not substitute the major elements because of a great difference in ionic radius and ionic charge and that tends to be enriched in the residual liquid of magmatic crystallization.

Radon (^{222}Rn) is a radioactive gas that may be emitted from any rock that contain radium (^{226}Ra), one of the products of the chain decay of ^{238}U (Ball et al., 1991; Keller et al., 1992; Ielsch et al., 2001). Even if it is frequently found at high levels in areas where there are no uranium mineralizations, however, in general, more radon is produced from rocks with high uranium content than from those with low content. Radon is a member of the inert, or noble, gas series (helium, argon, neon, xenon, krypton and radon). It has a very low chemical reactivity and under normal natural conditions it is an unreactive, colourless gas (boiling point 211 K, −62 °C) with a density almost eight times greater than that of air. The radon values for a given region are likely to be the result of a combination of properties of the underlying bedrock and soil, such as uranium and radium distribution, porosity, permeability, moisture content and weather conditions. The short half-life of ^{222}Rn (3.82 days) precludes slow transport over great distances, and thus it is believed that it occurs in the near-surface environment due to either in situ production in the surrounding soil or to CO_2 advective transport along permeable faults, depending on local conditions, such as permeability, soil moisture conditions, etc. (e.g., Toutain and Baubron, 1999; Baubron et al., 2002).

A lot of work has been done over the years studying the relationships of health hazards (especially, lung cancer) and Rn levels in mines and dwellings. However, recently, the investigation has been addressed to the determination of how closely correlations can be established between the levels of Rn prevailing at a specific location and the general levels expected in an area on geological and soil grounds (Webster, 2000).

The main relationships between natural or anthropogenic radionuclides and their retention/mobility in soils are well documented in the literature (e.g., Greeman et al., 1999; Kabata-Pendias, 2001; Barnett et al., 2002; Reimann et al., 2003). In order to increase the knowledge of the links between radioactivity values and soil features, a designed survey has been carried out in the area around Cecita Lake (Sila Grande, Calabria, Southern Italy). To achieve our aim, disintegrations contributed by K, Th, U and Rn, measured respectively in % (K), ppm (Th and U), and kBq/m^3 (Rn), have been related to soil units with well known general features. The data have been analysed by using graphical and numerical statistical procedures able to manage compositional data in their correct sample space. The paper summarises the results of the research and highlights the conclusions drawn. To our knowledge this is the first time that radioactivity data are considered as compositional data.

2. Area and soils description

2.1. Geological setting

The Sila Unit, which represents the bulk of the Sila Grande massif (Fig. 1a and b), is the uppermost Alpine thrust nappe in the northern sector of the Calabria–Peloritan Arc (CPA) (Amodio-Morelli et al., 1976; Van Dijk et al., 2000). It consists of three different Variscan metamorphic complexes (Gariglione, Mandatoriccio and Bocchigliero complexes), respectively representing high-, medium- and low-grade metamorphic facies, and of late-Variscan plutonites intruding them and forming the Sila batholith (Messina et al., 1991). This crystalline basement is discontinuously covered by Mesozoic (Triassic to Liassic) sedimentary units represented by the Longobucco group (Roda, 1964; Critelli, 1999).

The batholith consists of multiple intersecting, syn- and post-tectonic intrusions, ranging in length from several kilometres to less than 1 km. They have heterogeneous texture and composition from gabbro to leucomonzogranite, with prevailing tonalite and granodiorite. These intrusions were chronologically emplaced from more basic to acidic types at medium to shallow crustal levels. Centimetre- to metre-sized metamorphic xenoliths, similar to the adjacent country rocks, are found in the plutonites, except in the most leucocratic types. The entire batholith was generated from magma mixing processes involving mantle-derived magmas and heterogeneous crustal melts. The Sila magmatic suite evolved by assimilation–fractional crystallization and mixing processes (Messina et al., 1991).

The Gariglione complex consists of a pre-Variscan deep-crust basement re-equilibrated to amphibolite facies during the Variscan time. Biotite–sillimanite–garnet-bearing gneisses and subordinate amphibolites are the most widespread rocks. The contact with plutonites is characterised by a network of dykes and produced an irregular amphibolite facies thermal aureole.

The Mandatoriccio and Bocchigliero complexes crop out in the north-eastern area of the Sila Unit: the former geometrically underlies the latter, and both are unconformably covered by the Longobucco succession, which mainly consists of siliciclastic turbidites. The Mandatoriccio complex is composed of greenschist to amphibolite facies metamorphic rocks, characterised by a polyphasic deformation and by a metamorphic evolution. The Bocchigliero complex consists of low-grade metamorphic facies affecting a Paleozoic terrigenous–carbonatic–volcanic stratigraphic succession.

Various intramountane depressions of tectonic origin, such as the Cecita Lake basin, characterise the landscape of the Sila Grande massif. It consists of wide, dissected limbs of paleosurfaces (relict planation landforms) cut across the crystalline basement rocks and the

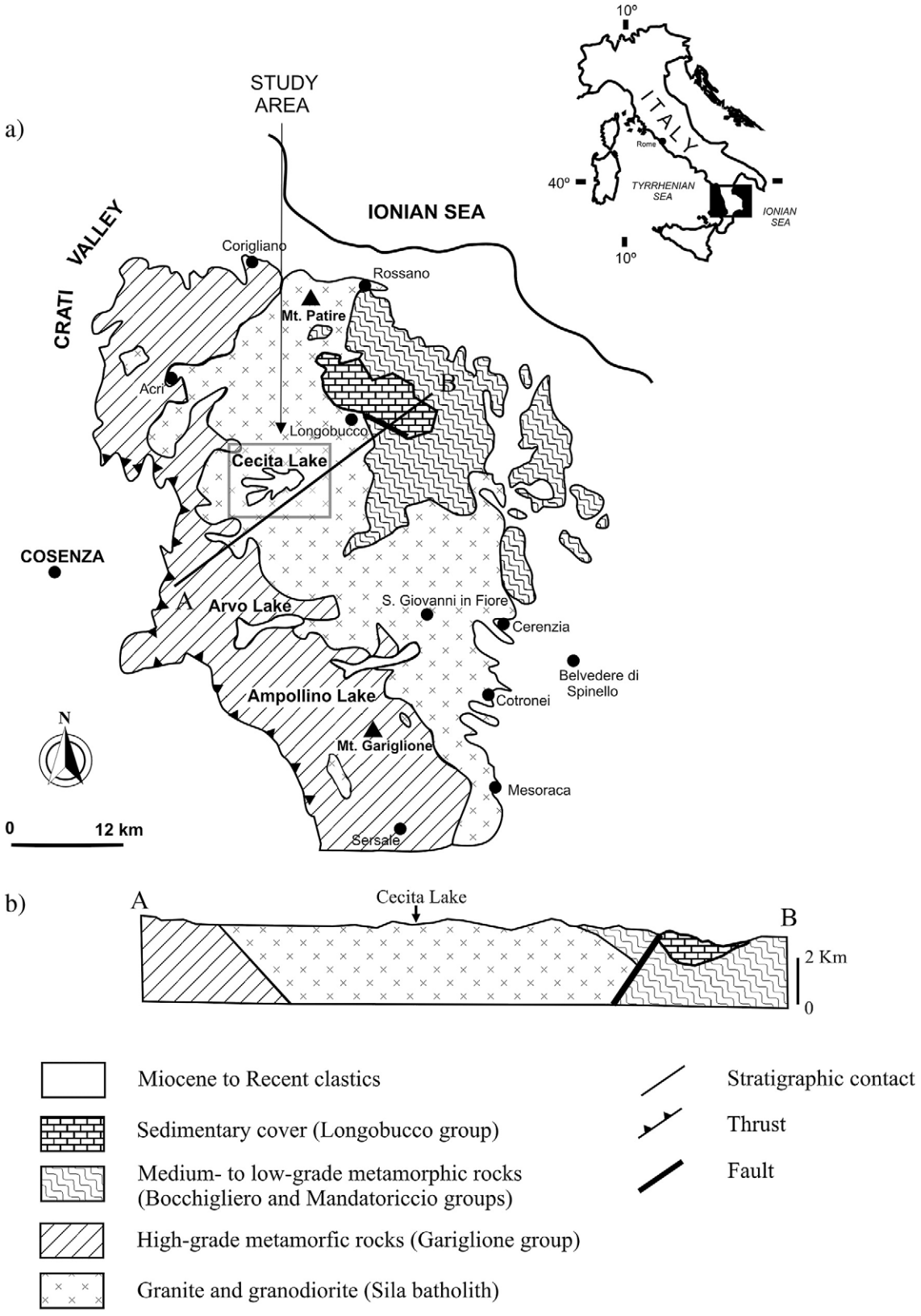

Fig. 1. (a) Location map of the study area (after Messina et al., 1991, modified) and schematic geological section (b) of the Sila Massif (after Liotta et al., 2008, modified).

sedimentary cover (e.g., Sorriso-Valvo, 1993; Molin et al., 2004), and displaced by tectonics above the present base-level at elevation ranges of 800–1700 m asl. Terraced fluvial and lacustrine deposits of Pleistocene age (ranging in size from gravels and sands to silts and clays, respectively) are morphologically entrenched within the older paleosurface landforms (e.g., Scarciglia et al., 2005). The main fault systems controlling the morphostructural evolution of this area are related to the main regional-scale tectonic structures and alignments (Van Dijk et al., 2000; Galli & Bosi, 2003; Tansi et al., 2007). They are orientated along NW–SE, NNW–SSE to N–S, and NE–SW directions

and influence the present-day hydrographic pattern, including the articulated shape of the Cecita Lake basin (Fig. 1) (Lulli and Vecchio, 2000; Galli and Bosi, 2003).

2.2. Soil description and mineralogical analysis

Previous works about soils in the study area show a large variety of soil types within the major taxonomic orders (Fig. 2) (Lulli and Vecchio, 2000; ARSSA, 2003; Scarciglia et al., 2005), despite the homogeneous bedrock and related sediments derived from the weathering of granite materials. This variability can be ascribed to the different response of soil-forming processes to relief characteristics (strongly controlled by tectonic history) and associated morphodynamic processes, climatic oscillations throughout the Pleistocene and the Holocene, vegetation cover and land-use changes often influenced by man's practices, and intrinsic erodibility factors of soil types according to their specific properties and substrata.

Most of the soil types outcropping in the Cecita Lake surroundings belong to the Entisol and Inceptisol orders (USDA, 2006), representing relatively young, poorly to moderately differentiated soils strongly dependent on the nature of the parent rock and the climatic conditions. Among the dominant pedogenetic processes there is the accumulation of organic matter in upper A horizons (umbric epipedon, USDA, 2006) without its downward migration within the profile, in response to progressive decomposition of primary vegetal tissues by bacterial activity. Organic matter content is on the average of 5–6%, sometimes approaching up to about 15%. Also a frequent rejuvenation of the weathering front occurs in soil profiles, due to important surface erosion by water runoff, especially on bare to scarcely-vegetated and steep slopes. Higher depth values of the umbric epipedon occur on flat terraces and paleosurface limbs: their mean values reach half a meter, with occasional thickness close to 1 m or more. In some protected flat landforms or topographic depressions, as well as along gentle footslope belts, severe reworking and accumulation of colluvial material eroded from upslope areas lead to the formation of thicker accretionary soil profiles. Sometimes soils appear buried by younger deposits (and associated soils) in response to morphodynamic processes. In particular, more developed but often buried and truncated Alfisols (USDA, 2006), exhibiting thick, rubified, argillic horizons (derived from clay illuviation into the subsoil) are limitedly preserved (usually below soils surface with different features) in the Cecita Lake surroundings. They testify for a different (pedo)climatic regime occurring in the past and for subsequent intense erosion (Lulli and Vecchio, 2000; Scarciglia et al., 2005).

Some specific pedologic features make the soilscape around Cecita Lake very peculiar. Upper A horizons often show the typical field appearance of volcanic soils with *andic* properties (Andisols, USDA, 2006), such as dark brown to blackish colours, dry powdery aspect, friable and fluffy consistence, low bulk density, high porosity and water retention, thixotropy. Detailed chemical, mineralogical and

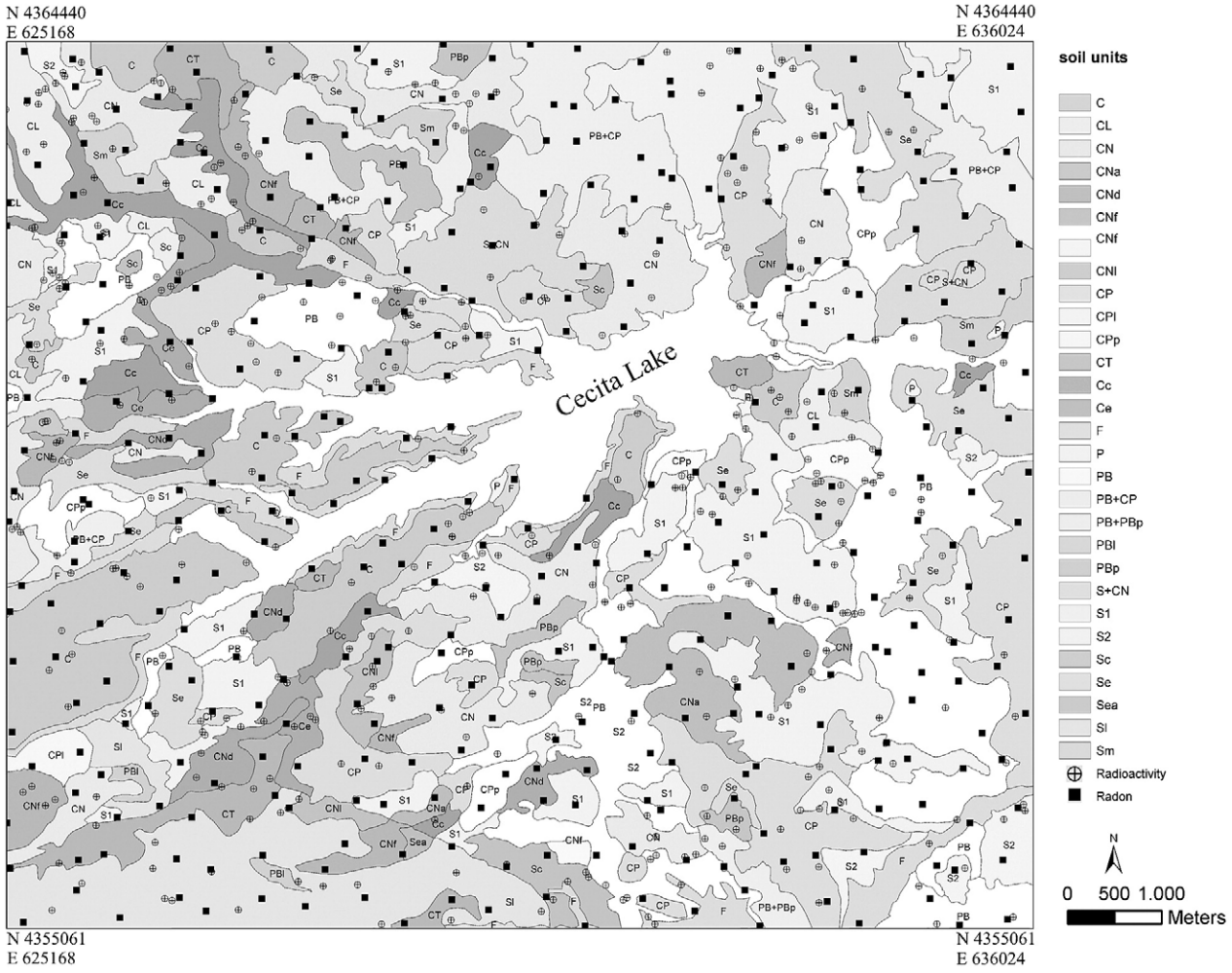

Fig. 2. Soil units recognised in the investigated area (see text for legend explanation) with location of radioactivity (circles) and radon (squares) measures.

micromorphological analyses recently demonstrated a contribution of windblown, fine volcanic glass during soil development, sourced by late Pleistocene(?) to Holocene high-energy volcanic eruptions from the Aeolian Islands. This material partly led to the neogenesis of some short-range order aluminosilicates (poorly-crystalline clay minerals), in turn producing the *andic*-like appearance of these soil horizons (Scarciglia et al., 2005, 2008).

The main primary components that occur both in bedrock and soil horizons as rock fragments or single crystals, consist of quartz, K-feldspar, plagioclase, and mica minerals. In particular, orthoclase and sometimes microcline occur, albite-twinned Na-plagioclase, biotite, and subordinate muscovite. Accessory minerals consist of amphibole, apatite, zircon, epidote, magnetite and sphene (Mirabella et al., 1996; Le Pera & Sorriso-Valvo, 2000; Le Pera et al., 2001).

Some representative soil samples were selected for scanning electron microscopy analysis (SEM-EDS) to identify which mineral species can be retained as potential sources of radioactivity. In particular, zircon (Fig. 3a), REE-phosphates (monazite-type) often rich in Th and U (Fig. 3b), and K-feldspar appear to be the main sources among primary minerals.

2.3. Soil series

All the soil units recognised and mapped in the Cecita Lake area have been grouped into 6 soil series, in turn subdivided into variant soil phases and additional units and a further soil group (Fig. 2), widely described in Lulli & Vecchio (2000) and hereinafter summarised.

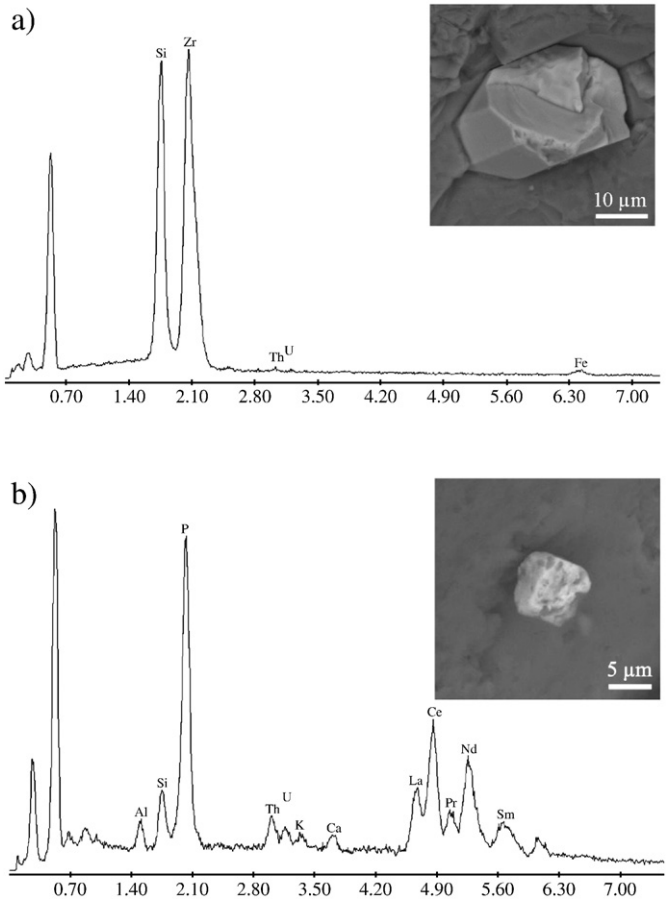

Fig. 3. SEM backscattered images and EDX spectra of zircon (a) and monazite (b) crystals.

2.3.1. Cecita Series

The soils belonging to this series developed mainly on gravels and sands of the terraced fluvio-lacustrine sedimentary infilling. Most of them can be classified as Pachic Haplumbrepts (USDA, 2006), usually characterised by deep profiles (A–Bw–2C), (very) dark brown colours, silt to sandy loam texture, high water holding capacity and good drainage conditions, acidic pH values, high organic matter content (reaching up to 10–13%). This series consists of the typic Cecita soil phase (C), the additional cumulic (Cc) and entic (Ce) phases, and the variant Cecita Lagarò (CL) and Cecita Tavullo (CT) ones.

2.3.2. Sila Series

This soil series includes soils developed on gently-rolling to flat or gently-inclined paleosurface limbs or morphological depressions cut across weathered plutonic and metamorphic basement rocks. They show moderately deep A–Bw–Cr-profiles, loam to sandy loam texture and dark brown colour. They are well-drained, with acid to subacid soil reaction and organic matter percentage around 3–5. In terms of Soil Taxonomy they can be considered as Typic Dystrochrepts and Typic Haplumbrepts (USDA, 2006). The Sila Series (S) can be subdivided into the typic Sila phases S1 and S2, as well as the additional cumulic (Sc), entic (Se), entic and steep (Sea), and lithologic (Sm) soil phases.

2.3.3. Colle dei Neri Series

The Colle dei Neri Series develops on steep slopes modelled on the plutonic and metamorphic bedrock. The soils have brown colour and thin profiles (Ap–A–(C)–Cr), poorly differentiated into soil horizons from the parent material and can be classified as Typic Udorthents (USDA, 2006). Their texture is loamy sand to sandy loam, their drainage conditions are good, pH ranges from slightly to moderately acid, organic matter never exceeds 5%. The Colle dei Neri Series is represented by the typic (CN), steep (CNa) and detritic (CNd) phases, coupled with the additional fluventic (CNf) and lithologic (CNl) ones. Very rare and limited outcrops of this soil series occur also on flat surfaces, showing intermediate features between the two end-members (S + CN).

2.3.4. Croce della Palma Series

The soils included in this series show thin, scarcely differentiated profiles with A-C(r)-types occurring on the crystalline basement rocks and/or the related detrital deposits, mainly on steep slopes. They are brown in colour, loamy sand to sandy loam in texture, low in amount of organic matter (always lower than 3%), with moderate to low water holding capacity and free drainage conditions. Soil reaction is weakly to moderately acid. From a taxonomic point of view they can be considered as Lithic Udorthents (USDA, 2006). Three soil phases can be distinguished within this series, such as the typic (CP), the lithologic (CPl) and the flat (CPp) phases.

2.3.5. Pietra Bianca Series

The soils forming the Pietra Bianca Series have thin, lithic soil profiles at early stages of pedogenetic evolution, developed on the same landforms of the Croce della Palma Series, but where erosive processes are particularly severe, pedogenetic processes have not been developed so much. Also many soil features are similar to the previous series (but less developed), and mainly form Lithic Haplumbrepts (USDA, 2006), grouped into the PB phase (typic), the PBl (lithologic) phase and the PBp (flat) phase. In places, soils with intermediate features between these latter two series occur (PB + CP).

2.3.6. Frisone Series

The soils of the Frisone Series are located on coarse to fine sediments of the fluvio-lacustrine infilling, mainly in the lowest lake terraces, the recent stream valleys and alluvial plains, and essentially belong to the Fluventic Haplumbrepts (USDA, 2006). They display moderately deep, typical A_1–A_2–2BC–2BCg profiles and greyish brown

colours, with moderate to high drainage conditions and similar water retention. Their texture ranges from silty loam to sandy loam, their pH shows slight to moderately acidic values, organic matter content is generally high. The Frisone Series consists of the sole typic phase F.

2.3.7. Paleosols on fluvial terraces

A further group (indicated as P) is represented by buried and/or surface but truncated paleosols developed on fluvial terraces. They are poorly widespread, scattered soils forming A–2Bt–2C(B)t-like profiles, on sand and gravel deposits of the lake infilling. Among the diagnostic features there is the deep argillic (Bt) horizon, allowing them to be classified as Alfisols (USDA, 2006), where organic matter is equal or lower than 1% (in contrast with the upper A horizon, approaching about 3–5%). The soils of this group are mainly loam to sandy loam in texture (but showing clay increase up to about 25–35% in the argillic horizon/s), moderately drained, weakly to moderately acid, and reddish in colour due to iron oxi-hydroxide staining.

All the soil units identified have been finally clustered into 13 groups on the basis of the similar dominant features (according to the soil series and soil complexes proposed by Lulli and Vecchio, 2000), to facilitate the statistical analysis and interpretation of radioactivity data in respect of soil properties and behaviour, as follow: 1 (C + Cc + Ce), 2 (CL), 3 (CT), 4 (CN, CNa, CNd, CNI), 5 (CNf), 6 (CP, CPI, CPp), 7 (F), 8 (PB, PBI, PBp, PB + PBp), 9 (S1, Sc, Se, Sea, Sm), 10 (S1, S2), 11 (PB + CP), 12 (S + CN), 13 (P). Result has been reported in Fig. 4.

3. Materials and methods

3.1. Radioactivity measurements

A soil-radioactivity regional survey (~4 samples/km^2) was carried out to study the relationships between soils and K, Th and U radioactivity values in the Cecita Lake basin, an area of about 105 km^2, in which about 400 samples were taken in the period from June to July 2004 (Fig. 2). Sampling sites were positioned by means of a GPS and measurements of natural radionuclides in the field were done using a GRM-260 gamma-ray spectrometer. The measurement is based on the capture of emitted gamma quanta in the scintillation detector. The gamma quanta of characteristic energies are transformed into electric pulses with heights that are proportional to the energies. The queue of electric pulses is consequently analyzed and separate pulses are sorted into individual channels of the measured spectrum. The spectrum of the GRM-260 spectrometer consists of 256 channels with a channel width of 12 keV. The spectrum is divided into four parts – groups of channels called ROI (region of interest) – with respect to the peak positions of studied radionuclides, due to the real resolution of the scintillation detector.

Radioactivity of rocks is usually caused by one of three natural sources of gamma-radiation: potassium, uranium and thorium. Each of those elements in natural conditions contains a fraction of radionuclide that can be detected in either direct or indirect way. The isotope ^{40}K emits gamma-rays with energy of 1.461 MeV, thus the determination of K is

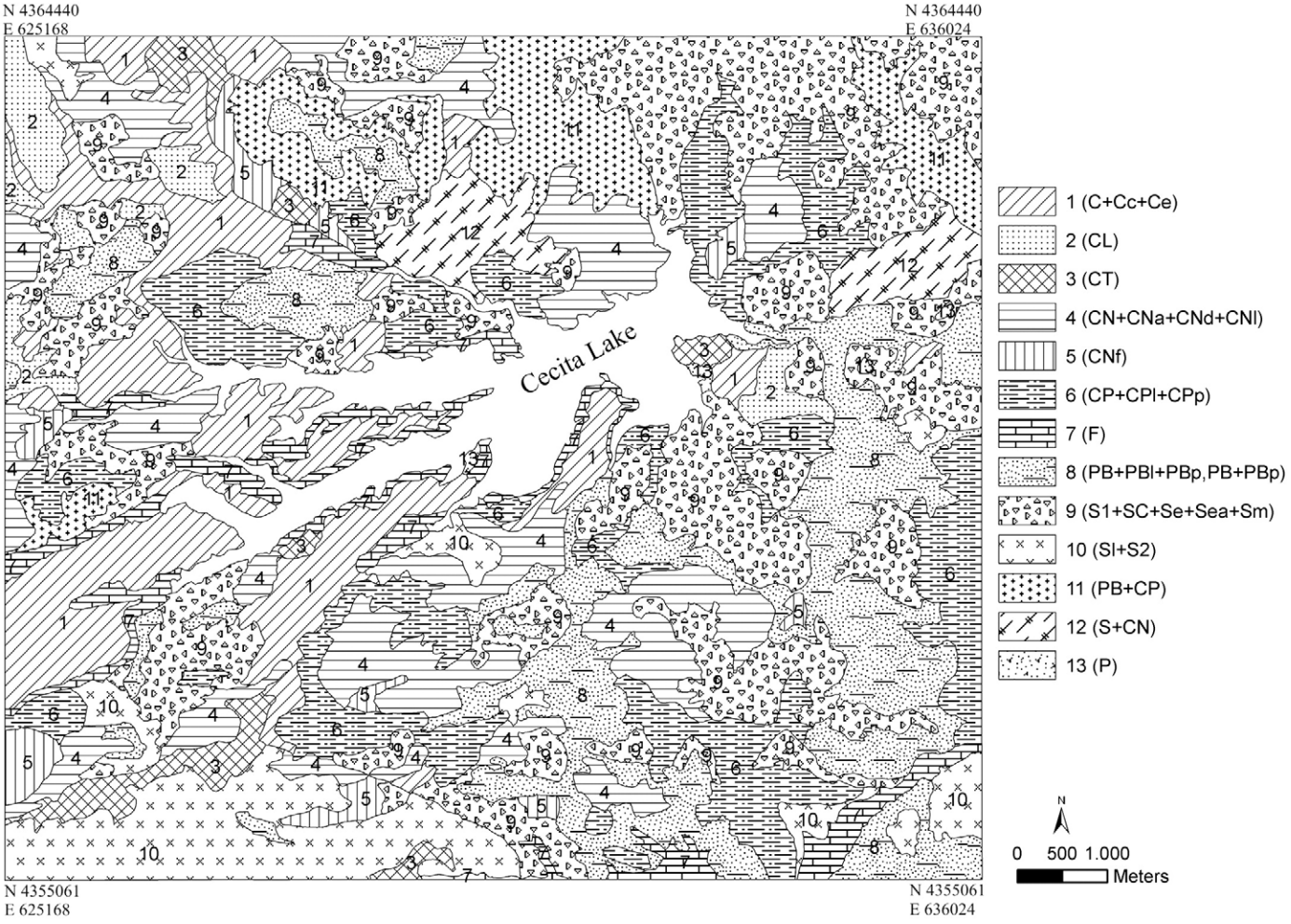

Fig. 4. Results of the clustering of the different soil units of Fig. 2 in 13 groups on the basis of the similar dominant features.

considered as direct. The concentration of K is given in mass percentage. The determination of U is based on the detection of the ^{214}Bi radionuclide, which is a member of the ^{238}U decay series emitting the energy of 1.764 MeV. In the case of U, the detection is therefore indirect and the concentration is given in ppm eU (equivalent of uranium). The determination of Th contents is indirect as referred to the ^{208}Tl radionuclide, with energy of 2.615 MeV, originating from the ^{232}Th decay series. The concentration of Th is given in ppm eTh.

3.2. Radon measurements

The spatial experimental design carried out to investigate the relationships between soils and experimental Rn values was carried out during June and July 2000, as shown in Fig. 2.

Soil gas samples have been collected with a probe driven into the ground to a depth of 1.0 m ca, so that measurements were not affected by atmospheric variations. Surface features (oscillations of the ground water-table, changes of climatic parameters and related pedoclimatic responses, etc.) that influence soil gas distribution provide a truly random component that makes soil gas interpretation a hard issue (Nazaroff, 1992; Oliver and Badr, 1995; Oliver and Khayrat, 2001). However, the standardisation of sampling conditions, the collection of a large number of samples and an appropriate statistical treatment of data can lead soil gas methods to be powerful tools for geological investigation (Klusman, 1993). Accidental soil gas variations can be minimised by sampling in short and dry periods. Our soil gas survey was performed during summer months characterised by relatively stable temperature, rainfall and moisture, thus minimising the climate effect on soil gas distribution (Hinkle, 1994).

Alpha activity of soil gas radon samples was measured in laboratory using the alpha-scintillation properties of silver activated zinc sulphide (Lucas, 1957; Semkow et al., 1994), using the Pylon AB-5 instrument. The latter was calibrated using a radioactive source of Ra-226 (model 3150A, Calibration standard), having an equilibrium activity with Rn-222 of 222.96 kBq/m^3 with an efficiency $E=74.5\%$. The soil gas was collected via a drying tube and aerosol filter into evacuated Lucas scintillation cells (which are suitable for detecting low levels of radon), having nominal volumes of 270 cm^3. An air-flux of 50 cm^3 s^{-1} is provided by an internal pump. Lucas cells were also calibrated, and according to the instrument calibration they have an efficiency $E=75\%$ and a sensitivity $S=3.65\%$. The gas sample was analysed in the laboratory about 3.5 h after its collection, so that the radioactive equilibrium could be achieved. In such a way, the "noise" of other isotopes with alpha-radiation emission in the decay was avoided (Rosner and Winkler, 2001; Ruckerbauer and Winkler, 2001; Winkler et al., 2001a,b).

4. Results and statistical analysis

In many geological data sets the variables are not entirely independent but are constrained to form a constant sum. Chemical analysis and concentrations data represent the most obvious example and great care must be applied when inspecting such constant-sum data (Aitchison, 1986). Radioactivity measurements corresponding to the presence of K, Th and U in the investigated matrices, where all the variables are expressed in the same relative units, have been managed as a sub-composition by log-contrast analysis. Values of the log-contrast equations were discriminated by considering the membership, a priori known, to the 13 defined soil groups (Buccianti and Pawlowsky-Glahn, 2005). Notched box-plots were used to visualise results by considering as categorical variable the soil groups, while the statistical tests of Kruskal–Wallis and median were applied to evaluate the presence of significant differences ($p<0.05$). By considering Rn measurements, since that element is the only variable obtained during the regional survey which is expressed in kBq/m^3, the logarithmic transformation was considered sufficient (Sinclair, 1991). The investigation of the shape of the frequency distribution of the variate was performed with the aim to point out the presence of more than one set of data, potentially cross-correlated with the soil unit groups a priori defined.

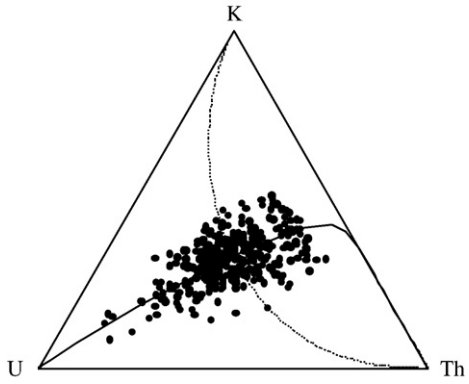

Fig. 5. Log-contrast analysis of the sub-composition U–K–Th; continuous and dotted lines represent the linear processes associated with the first and second log-contrast, respectively.

4.1. Potassium, thorium and uranium radioactivity values

The results of the K radioactivity measurements (372 values) range from a minimum of 0.13 to a maximum of 5.68%. A tendency of observations with lower values to group in the southern–western corner of the area is also revealed, while higher values tend to show a wide spatial dispersion. U radioactivity results (372 values) range from a minimum of 0.01 to a maximum of 19.01 ppm. However, most of the data show values lower than 9.51 ppm and high values are isolated outliers mainly located in the eastern part of the area. These observations can be responsible for the high variability of short spatial range. Th radioactivity (372 values) data range from a minimum of 0.64 to a maximum of 34.24 ppm with values widely variable and scattered within the whole area.

The simultaneous behaviour of the three variables expressed in percentages has been investigated from a graphical and numerical point of view by considering the ternary simplex as reported in Fig. 5 where the curves associated to the linear pattern of the first (continuous line) and second (dotted line) log-contrast equations have been reported (Aitchison, 1999). The corners of the ternary diagram are at 100% of the pure component end-members in the sub-composition and the points represent all the available experimental measures.

The first log-contrast is able to explain about 82.4% of the total data variability and consequently its equation appears to model what happened in the sub-composition, that is the compositional changes in uranium in comparison with a more or less constant ratio between K and Th.

The equation of the first log-contrast is given by:

$$+0.81\log(U)-0.47\log(\mathrm{Th})-0.34\log(K)=k_1,$$

or by considering that the coefficients are roughly in the ratios of 2:1:1 the following form, similar to the Law Mass Action, can be considered:

$$+2\log(U)-\log(\mathrm{Th})-\log(K)=k_1.$$

The presence of a near-constant log-contrast arises from the near-zero second eigenvalue, $\lambda_2=0.0042$ that allows to write the equation:

$$-0.74\log(K)+0.08\log(U)+0.67\log(\mathrm{Th})=k_2.$$

In this case too, the fact that the coefficients are roughly in the ratios of 9:1:8 suggest that a substantial simplification to our result can be performed as follows:

$$-9log(K) + \log(U) + 8\log(\mathrm{Th}) \cong \text{constant},$$

where the constant value is estimated from the sample average of the log-contrast.

In Fig. 6 notched box-plots of the first log-contrast values in the defined soil groups are reported. In a notched box-plot the notches represent a robust estimate of the uncertainty about the medians for box-to-box comparison. Boxes whose notches do not overlap indicate that the medians of the two groups differ at the 5% significance level (McGill et al., 1978). In this framework, less negative values are generally associated with higher U contents. Kruskal–Wallis and median tests allow accepting the null hypothesis ($p>0.05$) so that the presence of significant differences among them has to be ruled out. As a conclusion it is possible to say that fluctuations of the first log-contrast occur around a common median value, independently from the soil groups. Notwithstanding this result, the behaviour of groups 12 (S + CN) and 13 (P) (less negative values, higher U content) has to be noticed. Measurements in these cases are related to limited outcrops (Fig. 4) mainly located in the central part of the map, often near to the lake (group 13, P), and in its northern and eastern part. Soils of group 12 (S + CN) are rare: they occur on flat surfaces and are characterised by weakly to moderately differentiated profiles with intermediate amounts of organic matter (3–5%). Also soils of group 13 (P) are poorly widespread and scattered on flat surfaces (specifically on fluvial terraces, where they mainly outcrop along terrace scarps), but represent paleosoils often buried by younger soils or sediments. They exhibit more clayey texture in subsoil horizons due to clay illuviation, reddish colours produced by intense Fe-(hydr)oxide segregation and extremely poor organic matter content ($\leq$1%). Summarising, the statistical model related to the first log-contrast appears able to describe the high U variability and the consequent homogenisation of the differences potentially attributable to soil features; some exceptions can be evidenced, even if without significance, due to enrichments related both to presence of iron oxi-hydroxides and/or clay minerals (adsorption) and argillic horizons related to illuviation.

In Fig. 7 notched box-plots of the second log-contrast values in the 13 soil groups are reported. Less negative values are related to higher Th and lower K contents. Kruskal–Wallis and median tests allow to reject the null hypothesis ($p<0.05$), so that the presence of significant differences among them have to be here considered. In this context the behaviour of data in group 3 (CT), with less negative values, higher Th and lower K contents, has to be noticed, as well as in group 8 (PB, PBI, PBp, PB + PBp), showing more negative values, lower Th and higher K contents. These soil groups represent the two extreme situations described by the log-contrast. Soils of group 3 appear to outcrop in limited areas located in the northern and southern left part of the map; soils of group 8, on the contrary are more widespread and cover the map with a NW–SE pattern. In particular, group 3 represents highly differentiated and deep soil types with higher organic matter contents, developed on terrace surfaces, whereas group 8 consists of very thin soil profiles at early stages of pedogenic maturity, located along steep slopes and intensely eroded.

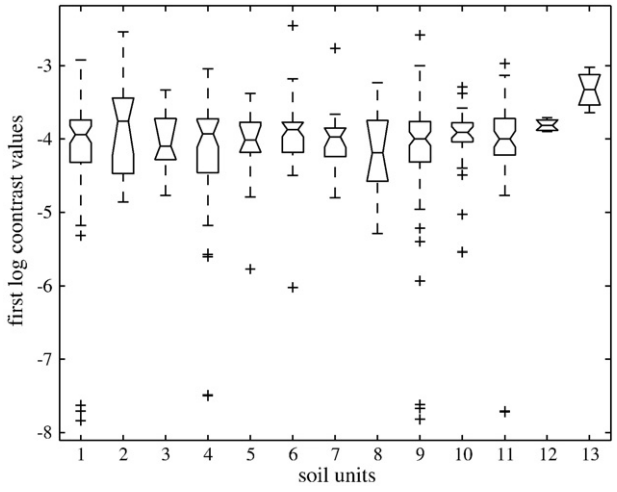

Fig. 6. Notched box-plots of the first log-contrast values discriminated by the a priori knowledge of sampling soil units (symbol + is associated to outlier and extreme values). Boxes whose notches do not overlap indicate that the medians of the two groups differ at the 5% significance level.

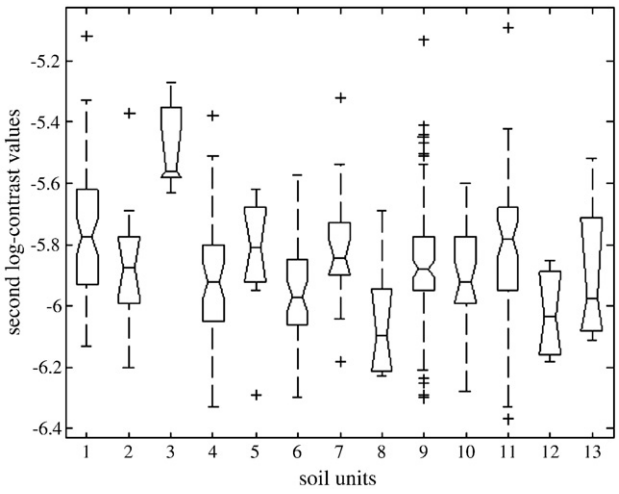

Fig. 7. Notched box-plots of the second log-contrast values discriminated by the a priori knowledge of sampling soil units (symbol + is associated to outlier and extreme values). Boxes whose notches do not overlap indicate that the medians of the two groups differ at the 5% significance level.

Summarising the results obtained by statistical investigation the most important features appear to be related to the absence for the first log-contrast of any discriminant effect of the soil groups due to the high U variability, a behaviour that can be explained in different ways for different soils characteristics (Fe-oxi-hydroxides, clays, organic matter presence and/or bedrock nature). On the other hand, when the Th/K ratio values are taken into account in the second log-contrast data, the discriminant effect of soil groups appears to be statistically significant, and soil groups 3 (CT) and 8 (PB, PBI, PBp, PB + PBp), appear to show a distinguishable behaviour.

4.2. Radon radioactivity values

Radon values (401 measurements) range from a minimum of 16.98 to a maximum of 55.76 kBq/m^3. The investigation of the frequency distribution (Fig. 8) indicates the clear presence of different groups of data and consequently the rejection of the null hypothesis about normality (Kolmogorov–Smirnov test, $p<0.01$). A comparison of the data discriminated by means of the a priori known soil groups, through notched box-plots summarised for groups of cases (Fig. 9), confirmed the possibility to clustering groups of soils with similar values as reported in Table 1. The application of Kruskall–Wallis and median tests confirmed that the chosen sets of data were characterised by high internal similarities ($p>0.05$) and that no other association led to a similar good answer. The cross-tabulation among the discovered four sets of data and the a priori known soil groups appears to be significant ($p<0.01$) confirming that radioactivity data attributable to Rn are clearly affected by the soil features, but not at the scale considered in the discrimination of the 13 soil groups. The

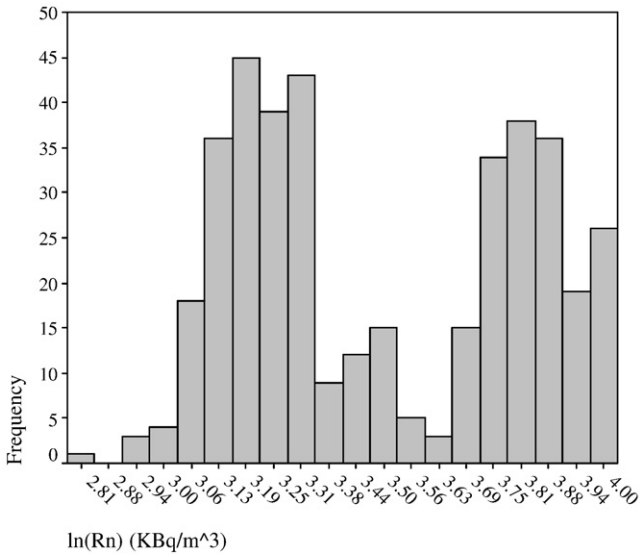

Fig. 8. Frequency distribution of the Rn logarithmic values.

spatial distribution of these data sets is reported in Fig. 10; it shows a rough correspondence between soil groups included in set I and thicker soil profiles, as well as between that included in set IV and thinner soils (Scarciglia et al., 2008).

5. Discussion

By considering the results of the previous analysis and the indications of statistical applications, it is clear that a defined association between soil features and U, Th and K contents is not revealed. On the contrary, Rn values show some relationship with soil evolution. From a general point of view, the modelling of the high U variability, well represented by the first log-contrast equation, reveals an element behaviour that tends to homogenise the experimental answer obtained from the a priori known different soil groups. Notwithstanding this condition, the discovery of the discriminative effect of the K/Th ratio values, shows a different situation for soil groups 3 (CT) and 8 (PB, PBI, PBp, PB + PBp). Finally, the clustering of the a priori known 13 soil groups in new 4 sets characterised by internal similarities for Rn values,

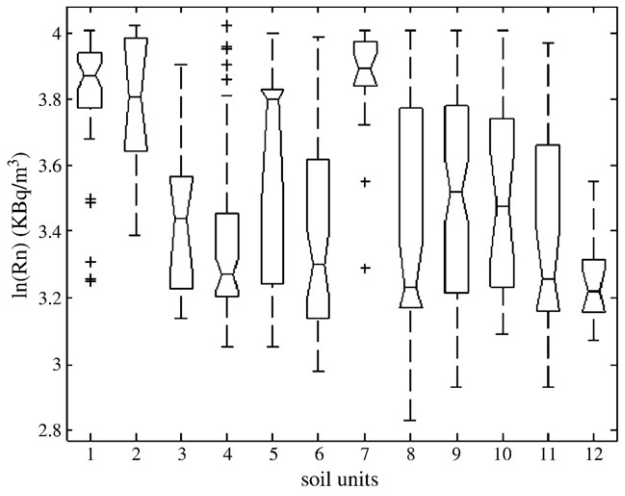

Fig. 9. Notched box-plots of the Rn values discriminated by the a priori knowledge of sampling soil unit (symbol + is associated to outlier and extreme values). Boxes whose notches do not overlap indicate that the medians of the two groups differ at the 5% significance level.

Table 1
Clustering of the a priori known soil groups in four different set of data characterised by internal similarities as deduced by the notched box-plots of Fig. 9 and the application of the median test ($p>0.05$).

Set of similar data	Soil groups (and corresponding associated soil units)	n	Minimum	Maximum	Median
I	1 (C + Cc + Ce) 2 (CL) 5 (CNf) 7 (F)	84	21.09	55.43	47.87
II	9 (S1, Sc, Se, Sea, Sm) 10 (S1, S2)	114	18.76	55.32	32.76
III	3 (CT) 4 (CN,CNa,CNd,CNI)	61	21.13	55.76	26.39
IV	6 (CP, CPI, CPp) 8 (PB, PBI, PBp, PB + PBp) 11 (PB + CP) 12 (S + CN)	142	16.98	55.13	26.12

Values are in kBq/m^3; n is the number of measures.

indicates that the features that have permitted to propose the original groups are too detailed to show differences in Rn values.

If the weathering of the homogeneous granitic bedrock is at the base of the genesis of soils developed in the investigated area, soil variability is mainly due to the geological and geomorphological setting, the Quaternary climatic oscillations and land-use changes (Reimer and Gundersen, 1989; Varley and Flowers, 1992; Scarciglia et al., 2005; Apollaro et al., 2009). However these conditions do not seem to have acted in a selected way in the investigated area, thus generating significant uranium enrichment from the parent rock to a specific soil. In this framework, a possible explanation may be found in the relatively young degree of pedogenetic development, and the strong resistance to weathering of many minerals containing uranium (Reimann et al., 2003). A further process able to promote diffusion in the area in more or less homogeneous way may be related to the change in the redox potential, which may promote the release of the uranyl cation $(UO_2)^{2+}$, thus favouring its transport in solution through groundwater, as well as its re-precipitation in reducing conditions (Vogel et al., 1999). In this context, group 13 (P), showing the higher U content, is characterised by buried Alfisols rarely outcropping along terrace scarps with very low content of humic matter and abundant Fe-oxi-hydroxides and clay minerals, thus suggesting that the element could have been enriched due to adsorption onto the latter components (Reimann et al., 2003), or to concentration into argillic horizons formed by pedogenic processes of clay particle illuviation. Group 12 (S + CN), given by Entisols and Inceptisols, is characterised by high U content too, but it is limitedly outcropping on flat surfaces and shows an overall poor to moderate soil development, with modest pedogenetic differentiation from the parent material and intermediate organic accumulation. In this case, the intermediate soil development suggests a possible partial enrichment related to pedogenesis and, in particular, to adsorption onto organic matter (Reimann et al., 2003), coupled with a significant contribution still sourced from the parent rock.

The spatial distribution of the uranium values reveals that high values are mainly located in the eastern part of the area and in some other scattered and small sites. These results can be explained taking into account the variable depth of topsoil horizons, as well as that of the granitic bedrock or sediments. In fact, the spatial distribution of soil thickness in the study area, shows that soils are thinner in the eastern sector, where the bedrock is consequently closer to, or exposed at, the topographic surface (Scarciglia et al., 2008), suggesting that the higher amounts of uranium are contributed by the granite parent materials. Despite the lack of data on natural radioactivity for the bedrock in the investigated area, due to its very scarce exposure at the topographic surface coupled with the dominance of granite-derived sediments of different types, some reference average values

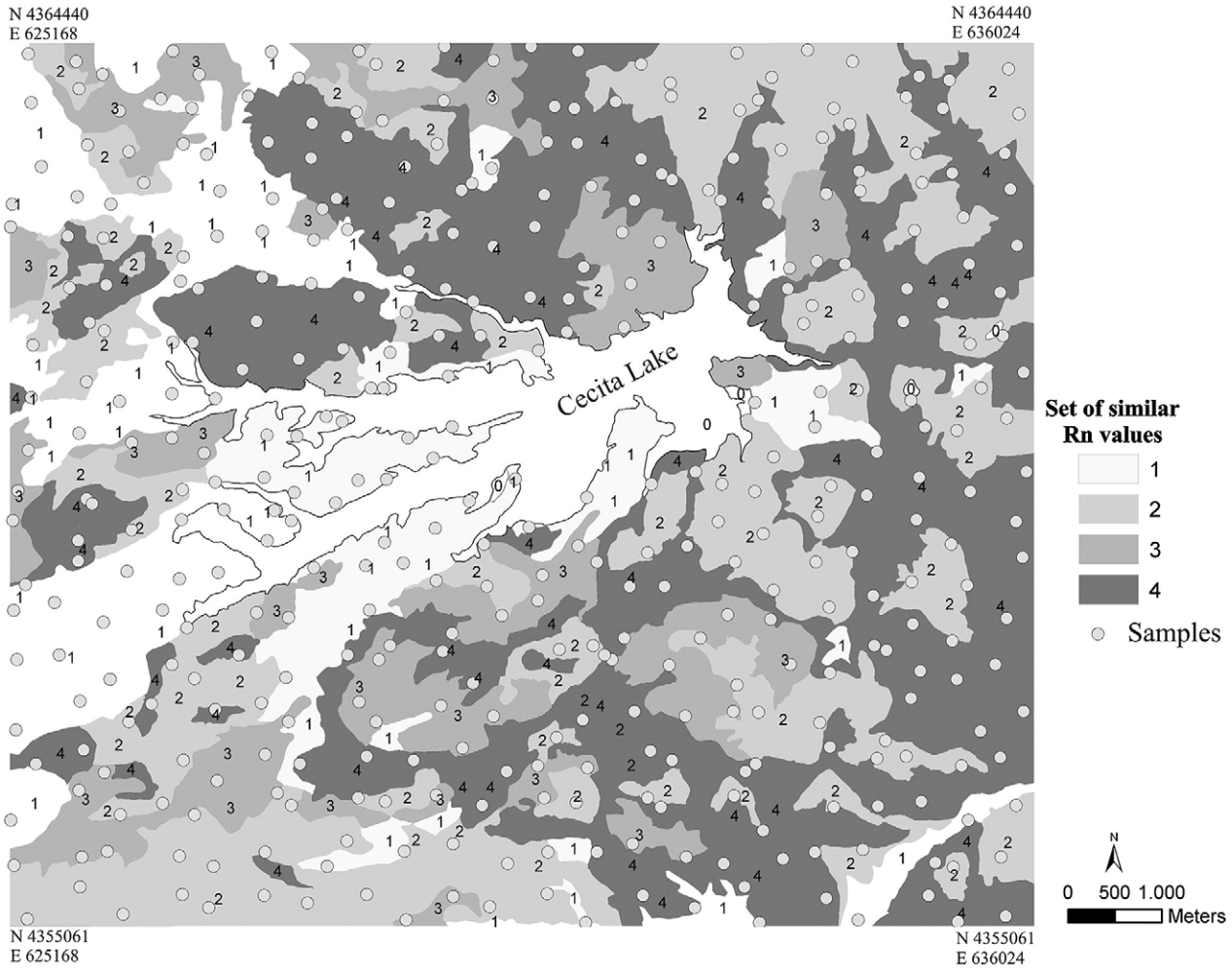

Fig. 10. Spatial distribution of the four clusters of soil groups obtained by associating similar measure values through box-plots analysis and subsequent application of the Kruskall–Wallis and median tests.

from analogous granitoids in surrounding areas can be considered, thus confirming our results. These values (U = 5.14 ppm, Th = 17.93 ppm, K = 4.56%, unpublished data), are very similar to those measured where the soil is extremely thin, and therefore the contribution of parent material is higher.

Soils of group 8 (PB, PBI, PBp, PB + PBp) notwithstanding the lower median value of the first log-contrast, are to some extent similar to those of group 12, although highly widespread and located on slopes; they represent Inceptisols at early stages of pedogenic maturity, very thin and low in organic matter, because of their topographic location and consequent severe erosion. Soils of group 3 (CT), showing low first log-contrast values too, are Inceptisols with deep, highly differentiated soil profiles and very rich organic matter content, limitedly outcropping on terrace surfaces.

The higher variability of the first log-contrast values for soil groups 1, 2, 4, 9 and 11 could be related to (i) an inhomogeneous physical weathering of the bedrock, (ii) the dominance of various sedimentary and reworking processes affecting the granite-derived material (see Section 2.2), (iii) the different thickness of soil profiles, (iv) the variable amount of organic matter and/or (iv) the consequent different degree of leaching.

Summarising, the first log-contrast analysis (modelling high U variability with respect to the K/Th ratio constant value), showing fluctuations that occur around a common median value, independently from the soil groups, appears to describe in a correct way the conditions previously discussed attributable to the combined effect of different processes.

By considering the second log-contrast values, groups 8 and 3 correspond, respectively, to very different soil types, representing the two extreme situations described by the statistical analysis, and show opposite Th and K contents, with lower Th and higher K in the former and higher Th and lower K content in the latter. As far as Th is concerned, it is present in the environment only in the oxidation state 4^+ and mainly occurs in primary minerals, such as zircon and REE-phosphates (see Section 2.2) or may sorb strongly to iron oxyhydroxides and humic matter (Nash and Choppin, 1980; Hunter et al., 1988; Murphy et al., 1999); consequently its behaviour, as other tetravalent actinides, is strongly affected by the presence of mineral and organic colloids (Lieser and Hill, 1992). This condition would be well represented by data of group 3 (CT), though the lack of correlation with other soil types suggests that pedogenetic thorium fractionation is not always efficient.

K content may be related both to primary minerals, that are abundant in granite rocks (K-feldspar, biotite and muscovite) and to neoformed phyllosilicate clay minerals of pedogenetic origin (namely illite, where K^+ represents the main cation in the lattice interlayer) (Apollaro et al., 2007a,b). In particular, where soil profiles are thinner and poorly differentiated into pedologic horizons as affected by severe erosion, a major contribution of potassium from the parent rock can be expected, a condition that appears to be well represented in data of group 8. In contrast, where they are more developed, this element can be

mainly retained in clay minerals. This is also consistent with the lower amounts of K where surface A horizons of soils are thicker (Scarciglia et al., 2008), such as those of group 3, as these layers are dominated by organic substances (and conversely by low amounts of primary minerals or neogenic clays).

Radon concentrations are related to the morphology that influenced the formation of the different soil units. The soils of the first unit (C + Cc + Ce) of the Cecita Series, developed mainly on gravels and sands of the terraced fluvio-lacustrine sedimentary infilling, have high radon values between 42.65 and 53.76 kBq/m^3, associated to the presence of topographic depressions, and, consequently, restricted atmospheric circulation and wind conditions. The highest radon concentrations were measured in the soils of the Frisone Series (typic phase F), located on coarse to fine sediments of the fluvio-lacustrine infilling (mainly in the lowest lake terraces), the recent stream valleys and the alluvial plains, and are characterised by high organic matter content. It is well known that organic substances and phosphates (the latter identified by scanning electron microscopy, see Section 2.2) may adsorb significant amounts of U (Reimann et al., 2003). In contrast, the soils of the group 4 (CN, CNa, CNd, CNI) of the Colle dei Neri Series, developed on slopes with different steepness (varying from gently-inclined paleosurfaces to steep slopes), have radon values ≤28.56 kBq/m^3. The soils of group 8 (PB, PBI, PBp, PB + PBp) of the Pietra Bianca Series, developed on steep slopes, have radon values ≤28.56 kBq/m^3, too. Consequently, from a general point of view, by considering the data of Table 1, radon values appear to be low along steep slopes, where soils are particularly thin, as a response to erosion, and where the bedrock itself may be exposed at surface; on the contrary, high radon values can be found on flat surfaces (which represent more stable sites in terms of geomorphic dynamics), where soils become thicker and more developed, so that also their capacity of adsorption onto their reactive sites (organic matter, clays and/or iron oxi-hydroxides) becomes higher; coherently, Greeman et al. (1999) have highlighted a very high affinity of Rn for organic matter. In addition, these soils generally show highly porous and aerated microstructures (Scarciglia et al., 2005, 2008), able to trap radon. In particular, the general trend of decrease in organic matter from soil group of set I to soil groups of set IV (also corresponding to a decrease of median Rn concentrations) suggests that organic substances and morphology play a prominent role in the sorption and retention of radon.

From a general point of view, the investigated area does not appear to present particular relationships among Rn radioactivity values and that of U, Th and K (cfr. Levinson and Coetzee, 1978; Card and Bell, 1982). Although the common source of radon is from small distances in the near-surface environment (caused by its short half-life and relatively low mobility), it is not to be excluded that it can be transported from deep hydrothermal systems: rising gas or water flows may enhance rapid radon exhalation towards the ground surface through host–rock porosity and discontinuities. Therefore, higher rates of measured Rn can be also related to the tectonic setting and spatial distribution of active faults, acting as preferential ways for carrying fluids, due to increased permeability in fractured rocks within or close to shear zones (e.g., Toutain and Baubron, 1999). A poor relationship between radon values and the NNW–SSE-trending normal fault bordering the Cecita Lake basin at its eastern end (Galli and Bosi, 2003), as well as with the frame of minor tectonic alignments that control relief features and patterns of the hydrographic network (see Section 2.1), seems to affect the lake surrounding, although not well-defined and partly masked by background concentrations.

6. Conclusions

Since radioactivity values measured on complex systems as soils are affected and perturbed by several mixed effects, a detailed investigation has been performed in the Cecita Lake basin (Sila Grande, Calabria, Southern Italy), with the aim to point out a potential relationship among soil properties and experimental data attributable to K, U, Th and Rn presence.

Disintegrations contributed by K, U, Th and Rn respectively in % (K), ppm (U and Th) and kBq/m^3 (Rn), have been related to 13 a priori known soil unit groups with well-defined general features and spatial position. The data have been analysed by using graphical and numerical statistical procedures able to manage compositional (proportional as %, ppm and so on) data by taking into account the correct sample space in each case. Compositional changes have been modelled in the simplex space by using log-contrast analysis, while the positive (∈ to the R^+ line) Rn radioactivity values, have been analysed after having applied the logarithmic transformation.

Our methodology has allowed to discover and model the most important feature of the investigated area given by the high U variability. This geochemical behaviour tends to homogenise the differences potentially attributable to soil features, with the exception of local situations where uranium could be enriched due to adsorption onto iron oxi-hydroxides and/or clay minerals or concentrated in argillic horizons due to illuviation. In this framework, the discriminative effect of the K/Th ratio values, has revealed the presence of soil groups where Th behaviour, as other tetravalent actinides, is strongly affected by the presence of mineral colloids or where the presence of clays affects the trapping of K, particularly when the contribution of the bedrock can be ruled out. Finally, the investigation of the shape of the frequency distribution for logarithmic Rn values has revealed that only one probability model (for example the Gaussian one) is not able to capture the mechanism that has generated the data. The presence of similar groups of data has been evaluated by comparing box-plots of the values related to the a priori known soil groups. The new four sets characterised by internal similarities for Rn values, as evaluated by statistical tests ($p<0.05$), have been mapped and cross-correlated with soil properties, thus revealing that morphology and organic content appears to be able to generate important discriminative effects. To our knowledge this is the first time that radioactivity data are managed in the correct sample space and the obtained results encourage to explore further this field of investigation proposing statistical models to be used in different natural environments.

Acknowledgements

This research has been financially supported by Italian MIUR (Ministero dell'Istruzione, dell'Universita' e della Ricerca Scientifica e Tecnologica), PRIN 2007, through project 2007M4K94A_002 (A.B.). The authors thank R. Olea and two anonymous referees for helpful reviews.

References

Aitchison, J., 1986. The statistical analysis of compositional data. Monographs on Statistics and Applied Probability. Chapman & Hall Ltd., London. Reprinted (2003) with additional material by The Blackburn Press, Caldwell, NJ.

Aitchison, J., 1999. Log-ratios and natural laws in compositional data analysis. Mathematical Geology 24 (4), 365—379.

Akerblom, G., Anderson, P., Clavensjo, B., 1984. Soil gas radon — a source for indoor radon daughters. Radiation Protection Dosimetry 7 (1), 49—54.

Amodio-Morelli, L., Bonari, G., Colonna, V., Dietrich, D., Giunta, G., Ippolito, F., Liguori, V., Lorenzoni, S., Paglionico, A., Perrone, V., Piccarreta, G., Russo, M., Scandone, P., Zanettin Lorenzoni, E., Zappetta, A., 1976. L'Arco Calabro Peloritano nell'orogene appenninico-maghrebide. Memorie della Società Geologica Italiana 17, 1—60.

Apollaro, C., Marini, L., De Rosa, R., 2007a. Use of reaction path modeling to predict the chemistry of stream water and groundwater: a case study from the Fiume Grande valley (Calabria, Italy). Environmental Geology 51, 1133—1145.

Apollaro, C., Marini, L., De Rosa, R., Settembrino, P., Scarciglia, F., Vecchio, G., 2007b. Geochemical features of rocks, stream sediments, and soils of the Fiume Grande Valley (Calabria, Italy). Environmental Geology 52, 719—729.

Apollaro, C., Accornero, M., Marini, L., Barca, D., De Rosa, R., 2009. The impact of dolomite and plagioclase weathering on the chemistry of shallow groundwaters circulating in a granodiorite-dominated catchment of the Sila Massif (Calabria, Southern Italy). Applied Geochemistry 24, 957—979.

ARSSA (Agenzia Regionale per lo Sviluppo e per i Servizi in Agricoltura), 2003. I suoli della Calabria. Carta dei suoli in scala 1:250000 della Regione Calabria. In: Rubbettino, et al. (Ed.), Monografia divulgativa: Programma Interregionale Agricoltura-Qualità — Misura 5, ARSSA, Servizio Agropedologia. Catanzaro, Italy, 387 pp.

Badr, I., Oliver, M.A., Hendry, G.L., Durrani, S.A., 1993. Determining the spatial scale of variation in soil radon values using a nested survey and analysis. Radiation Protection Dosimetry 49 (4), 433—442.

Ball, T.K., Cameron, D.G., Colman, T.B., Roberts, P.D., 1991. Behaviour of radon in the geological environment: a review. Quarterly Journal of Engineering Geology 24 (2), 169—182.

Barnett, M.O., Jardine, P.M., Brooks, S.C., 2002. U(VI) adsorption to heterogeneous subsurface media: application of a surface complexation model. Environtal Science & Technology 36 (5), 937—942.

Baubron, J.C., Rigo, A., Toutain, J.P., 2002. Soil gas profiles as a tool to characterise active tectonic areas: the Jaut Pass example (Pyrenees, France). Earth and Planetary Science Letters 196, 69—81.

Buccianti, A., Pawlowsky-Glahn, V., 2005. New perspectives on water chemistry and compositional data analysis. Mathematical Geology 37 (7), 703—727.

Card, J.W., Bell, K., 1982. Collection of radon decay products. A uranium exploration technique. Journal of Geochemical Exploration 17, 63—76.

Critelli, S., 1999. The interplay of lithospheric flexure and thrust accommodation in forming stratigraphic sequences in the southern Apennines foreland basin system, Italy. Accademia Nazionale dei Lincei, Rendiconti Lincei Scienze Fisiche e Naturali 10, 257—326.

Galli, P., Bosi, V., 2003. Catastrophic 1638 earthquakes in Calabria (southern Italy): new insights from paleoseismological investigation. Journal of Geophysical Research 108 (B1). doi:10.1029/2001JB001713 2004, 20 pp.

Greeman, D.J., Rose, A.W., Washington, J.W., Dobos, R.R., Ciolkosz, E.J., 1999. Geochemistry of radium in soils of the Eastern United States. Applied Geochemistry 14 (3), 365—385.

Hinkle, M.E., 1994. Environmental conditions affecting concentrations of He, CO_2, O_2, and N_2 in soil gases. Applied Geochemistry 9, 53—63.

Hunter, K.A., Hawke, D.J., Choo, L.K., 1988. Equilibrium adsorption of thorium by metal oxides in marine electrolytes. Geochimica et Cosmochimica Acta 52, 627—636.

Ielsch, G., Thieblemont, D., Labed, V., Richin, P., Tymen, G., Ferry, C., Robe, M.C., Baubron, J.C., Bechennec, F., 2001. Radon (Rn-222) level variations on a regional scale: influence of the basement trace element (U, Th) geochemistry on radon exhalation rates. Journal of Enrionmental Radioactivity 53 (1), 75—90.

Kabata-Pendias, A., 2001. Trace Elements in Soils and Plants, 3rd ed. CRC Press, Boca Raton, Fla. 413 pp.

Keller, G., Schneiders, H., Shutz, M., Siehl, A., Wiegand, J., 1992. Geological structure and geochemistry controlling radon in soil gas. Radiation Protection Dosimetry 45, 235—239.

Klusman, R.W., 1993. Soil Gas and Related Methods for Natural Resource Exploration. J. Wiley & Sons, New York. 483 pp.

Le Pera, E., Sorriso-Valvo, M., 2000. Weathering and morphogenesis in a Mediterranean climate, Calabria, Italy. Geomorphology 34, 251—270.

Le Pera, E., Arribas, J., Critelli, S., Tortosa, A., 2001. The effects of source rocks and chemical weathering on the petrogenesis of siliciclastic sand from the Neto River (Calabria, Italy). Sedimentology 48, 357—378.

Levinson, A.A., Coetzee, G.L., 1978. Implications of disequilibrium in exploration for uranium ores in the surficial environment using radiometric techniques— a review. Minerals Science and Engineering 10, 19—27.

Lieser, K.H., Hill, R., 1992. Hydrolysis and colloid formation of thorium in water and consequences for its migration behaviour: comparison with uranium. Radiochimica Acta 56 (1), 37—45.

Lima, A., Albanese, S., Cicchella, D., 2005. Geochemical baselines for the radioelements K, U, and Th in the Campania region, Italy: a comparison of stream-sediment geochemistry and gamma-ray surveys. Applied Geochemistry 20, 611—625.

Liotta, D., Caggianelli, A., Kruhl, J.H., Festa, V., Prosser, G., Langone, A., 2008. Multiple injections of magmas along a Hercynian mid-crustal shear zone (Sila Massif, Calabria, Italy). Journal of Structural Geology 30, 1202—1217.

Lucas, H.F., 1957. Improved low-level alpha scintillation counter for radon. The Review of Scientific Instruments 28 (9), 680—683.

Lulli, L., Vecchio, G., 2000. I suoli della Tavoletta "Lago Cecita" nella Sila Grande in Calabria. Monografia dell'Istituto Sperimentale per lo Studio e la Difesa del Suolo, Progetto PANDA, Sottoprogetto 2, Serie 1, Catanzaro, Italy. 78 pp.

McGill, R., Tukey, J.W., Larsen, W.A., 1978. Variations of boxplots. The American Statistician 32, 12—16.

Messina, A., Compagnoni, R., De Vivo, B., Perrone, V., Russo, S., Barbieri, M., Scott, B., 1991. Geological and petrochemical study of the Sila Massif plutonic rocks (northern Calabria, Italy). Bollettino della Società Geologica Italiana 110, 165—206.

Mirabella, A., Vecchio, G., Risi, B., 1996. Caratterizzazione mineralogica dei suoli su granito e micascisto in Sila Grande. Calabria Verde 2, 17—24.

Molin, P., Pazzaglia, F.J., Dramis, F., 2004. Geomorphic expression of active tectonics in a rapidly-deforming forearc, Sila Massif, Calabria, Southern Italy. American Journal of Science 304, 559—589.

Murphy, R.J., Lenhart, J.L., Honeyman, B.D., 1999. The sorption of thorium(IV) and uranium (VI) to hematite in the presence of natural organic matter. Physicochemical Engineering Aspects 157, 47—62.

Nash, K.L., Choppin, G.R., 1980. Interaction of humic and fulvic acids with Th(IV). Journal of Inorganic and Nuclear Chemistry 42, 1045—1050.

Nazaroff, W.W., 1992. Radon trasnsport from soil to air. Reviews of Geophysics 30 (2), 137—160.

Nelson-Eby, G., 2004. Principles of Environmental Geochemistry. Thomson Learning Inc.0-12-229061-5.

Nero, A.V., Gadgil, A.J., Nazaroff, W.W., Revzen, K.L., 1990. Indoor radon and decay products: concentrations causes, and control strategies. DOE/ER-0480P, Department of Energy, Office of Health and Environmental Research, Washington, D.C. In.

Oliver, M.A., Badr, I., 1995. Determining the spatial scale of variation in soil radon concentration. Mathematical Geology 27 (8), 215—218.

Oliver, M.A., Khayrat, A.L., 2001. A geostatistical investigation of the spatial variation of radon in soil. Computer and Geosciences 27 (8), 893—922.

Plant, J.A., Reeder, S., Salminen, R., Smith, D.B., Tarvainen, T., De Vivo, B., Petterson, M.G., 2003. The distribution of uranium over Europe: geological and environmental significance. Transactions of the Institution of Mining and Metallurgy section B-Applied Earth Science 112 (3), 221—238.

Reimann, C., Siewers, U., Tarvainen, T., Bityukova, L., Eriksson, J., Gilucis, A., Gregorauskiene, V., Lukashev, V.K., Matinian, N.N., Pasieczna, A., 2003. Agricultural soils in northern Europe: a geochemical atlas. Geologishes Jahrbuch Sonderhefte Reihe D, Heft SD 5, Hannover. 279 pp.

Reimer, G.M., Gundersen, L.S., 1989. A direct correlation among indoor Rn, and soil gas radon and geology in the Reading Prong near Boyertown, Pennsylvania. Health Physics 57 (1), 155—160.

Roda, C., 1964. Distribuzione e facies dei sedimenti neogenici nel Bacino Crotonese. Geologica Romana 3, 319—366.

Rosner, G., Winkler, R., 2001. Nuclide-dependent local and collector surface effects in sampling of radioactive deposition to ground. Applied Radiation and Isotopes 55 (6), 823—829.

Ruckerbauer, F., Winkler, R., 2001. Radon concentration in soil gas: a comparison of methods. Applied Radiation and Isotopes 55 (2), 273—280.

Scarciglia, F., Le Pera, E., Vecchio, G., Critelli, S., 2005. The interplay of geomorphic processes and soil development in an upland environment, Calabria, South Italy. Geomorphology 69 (1–4), 169—190.

Scarciglia, F., De Rosa, R., Vecchio, G., Apollaro, C., Robustelli, G., Terrasi, F., 2008. Volcanic soil formation in Calabria (southern Italy): the Cecita Lake geosol in the late Quaternary geomorphological evolution of the Sila uplands. Journal of Volcanology and Geothermal Research 177 (1), 101—117.

Semkow, T.M., Parekh, P.P., Schwenker, C.D., Dansereau, R., Webber, J.S., 1994. Efficiency of the Lucas scintillation cell. Nuclear Instruments and Methods in Physics Research A 353, 515—518.

Siegel, M.D., Bryan, C.R., 2005. Environmental geochemistry of radioactive contamination. In: Sherwood Lollar, B. (Ed.), Environmental Geochemistry. In: vol. 9 of Treatise on Geochemistry. Elsevier, pp. 205—262.

Sinclair, A.J., 1991. A fundamental approach to threshold estimation in exploration geochemistry: probability plots revised. Journal Geochemical Exploration 41, 1—22.

Sorriso-Valvo, M., 1993. The geomorphology of Calabria. A sketch. Geografia Fisica e Dinamica Quaternaria 16, 75—80.

Tansi, C., Muto, F., Critelli, S., Iovine, G., 2007. Neogene–Quaternary strike-slip tectonics in the central Calabrian Arc (southern Italy). Journal of Geodynamics 43, 393—414.

Toutain, J.P., Baubron, J.C., 1999. Gas geochemistry and seismotectonics: a review. Tectonophysics 304, 1—27.

USDA (United States Department of Agriculture), 2006. Keys to soil taxonomy, USDA, Soil Survey Staff, Natural Resources Conservation Service, Washington D.C., 10th ed. 333 pp.

Van Dijk, J.P., Bello, M., Brancaleoni, G.P., Cantarella, G., Costa, V., Frixa, A., Golfetto, F., Merlini, S., Riva, M., Torricelli, S., Toscano, C., Zerilli, A., 2000. Tectonophysics 324, 267—320.

Varley, N.R., Flowers, A.G., 1992. Radon and its correlation with some geological features of the south-west of England. Radiation Protection Dosimetry 45 (1–4), 245—248.

Vogel, J.C., Talma, A.S., Heaton, T.H.E., Kronfeld, J., 1999. Evaluating the rate of migration of an uranium deposition front within the Uitenhage Aquifer. Journal of Geochemical Exploration 66, 269—276.

Webster, R., 2000. Is soil variation random? Geoderma 97, 149—163.

Winkler, R., Ruckerbauer, F., Bunzl, K., 2001a. Radon concentration in soil gas: a comparison of the variability resulting from different methods, spatial heterogeneity and seasonal fluctuations. Science of the Total Environment 272 (1), 273—282.

Winkler, R., Ruckerbauer, F., Trautmannsheimer, M., Tschiersch, J., Karg, E., 2001b. Diurnal and seasonal variation of the equilibrium state between short-lived radon decay products and radon gas in ground-level air. Radiation and Environmental Biophysics 40 (2), 115—123.